

# Green Synthesis of Copper Oxide and Zinc Oxide Nanoparticles from *Crossandra infundibuliformis* Extract and its Antibacterial Application in Wound Dressing Films

Arunavarsini K<sup>1</sup>, Sekar M<sup>2</sup>, Yuvansasi V<sup>3</sup>, Achuth J<sup>4</sup>, Mahenthiran R<sup>5</sup>

<sup>1</sup>PhD Scholar, Department of Microbiology, Dr. N.G.P. Arts and Science College, Coimbatore-641048, Tamil Nadu, India.

<sup>2,3</sup>PG Students, Department of Microbiology, Dr. N.G.P. Arts and Science College, Coimbatore-641048, Tamil Nadu, India.

<sup>4</sup>Assistant Professor, Department of Microbiology, Hindusthan College of Arts and Science, Coimbatore-28.

<sup>5</sup>Assistant Professor, Department of Microbiology, Dr. N.G.P. Arts and Science College, Coimbatore-641048, Tamil Nadu, India.

## Abstract

Plant extract-based green production of metal oxide nanoparticles is a viable substitute for the conventional chemical synthesis approach. This biogenic process can be scaled up rapidly and executed at room temperature and pressure. The current work compares the antibacterial activity of chemically manufactured copper oxide and zinc oxide nanoparticles with those produced using a plant extract from *Crossandra infundibuliformis*. Furthermore, the study also encompasses the preparation of wound dressing films using the developed nanoparticles and the evaluation of their potential antimicrobial properties. The optical characterization of the synthesized nanoparticles exhibited an absorption peak of 574 nm and 333 nm with corresponding mean sizes of 50 nm and 40 nm for copper oxide and zinc oxide nanoparticles, respectively. The highest zone of inhibition by both the nanoparticles against *Pneumoniae*, followed by *S. epidermidis*, *S. aureus* and *P. aeruginosa*. Both the nanoparticles tested for the determination of their minimum inhibitory and minimum bactericidal concentrations exhibited significant activity towards the test pathogens. The wound dressing film developed utilizing the nanoparticles displayed a considerable zone of inhibition against the pathogens. Therefore, it could be ascertained from the work that nanoparticles synthesized through biogenic routes tend to exhibit substantial antibacterial activity.

**Keywords:** Nanoparticles, *Crossandra infundibuliformis*, Zinc oxide, Copper oxide, Antibacterial

## 1. Introduction

The complexity of wound-healing processes and the need for regulating conditions outside of clinical settings have made managing wounds increasingly challenging in recent years. A wound dressing's primary purpose, aside from providing protection, is to expedite the healing process. Modern wound

dressings are made to keep patients from drying out and promote healing by serving as delivery systems for bioactive ingredients. (Gupta et al., 2010; Boateng & Catanzano, 2015b). The complexity of wound-healing processes and the need for regulating conditions outside of clinical settings have made managing wounds increasingly challenging in recent years. A wound dressing's primary purpose, aside from providing protection, is to expedite the healing process. Modern wound dressings are made to keep patients from drying out and promote healing by serving as delivery systems for bioactive ingredients (Zhang et al., 2017b; Gil et al., 2012). Antibiotics, nanoparticles (metal and metallic oxides and light-induced antibacterial agents), cationic organic agents, and other types of antibacterial agents can all be included in the dressing to significantly enhance prevention of infections (Kaya et al., 2018; Martinotti and Ranzato, 2018).

Several forms of nanomaterials, including nanoparticles, nanospheres, nanocapsules, nanoemulsions, nanocarriers, and nanocolloids, can be developed for the treatment of wound infections. (Niska et al., 2018). In the last ten years, there has been a surge in the application of metals and metal nanoparticles to combat infections. As a result, a large number of metal nanoparticles have been commercialized and utilized in hospitals as a coating for wound dressings. (Ficai et al., 2014). Since metal ions have a unique chemistry that permits them to interact with crucial functional groups in biological molecules, they have a wide range of antibacterial activity against many cellular targets (Lemire et al., 2013). Metals, depending on their intrinsic properties, can target distinct functional groups on metabolites, proteins, nucleic acids, lipids, and carbohydrates that can culminate in a detrimental cascade of reactions within the cell (Li et al., 2017). A few of the resulting consequences include disruption of the electron transport chain, protein dysfunction and denaturation affecting metabolism, redox imbalance, inhibition of DNA replication and repair, altered membrane potential and solute transport, DNA damage and conformation changes, and carbohydrate degradation (Slavin et al., 2017a).

The synthesis of bioactive nanoparticles for a variety of biomedical applications is becoming easier, faster, more cost-effective, and more yielding with the use of phyto-nanotechnology, which employs extracts from plant parts (such as roots, leaves, barks, fruits, etc.) (Thakkar et al., 2010; Ahmad et al., 2019). When reacting with metal oxides, the phytochemicals present in plants serve as reducing or capping agents, and these methods significantly improve the nanoparticle synthesis protocol, yield, product bioactivity, and functionality while simultaneously ensuring that the entire process is eco-friendly. Plant-derived phytochemicals operate as reducing or capping agents when they react with metal oxides. These techniques greatly enhance the yield, bioactivity, and efficiency of the final product while ensuring an environmentally benign approach. (Al-saggaf, 2021). Green synthesis has played a significant part in stabilizing bioactive nanoparticles, which could mitigate their detrimental impact on human cells and increase their potential for use in the treatment of human diseases (Batoool et al., 2020).

*Crossandra Infundibuliformis* is an indigenous plant found in Sri Lanka, Malaysia and Southern India and belongs to the Acanthaceae family. It has been demonstrated to have a number of therapeutic benefits and is used to treat a variety of diseases (Dave et al., 2021). It has been reported that the leaf extract of *Crossandra Infundibuliformis* possesses larvicidal, antibacterial, and antioxidant properties (Elamathi et al., 2011; Madhumitha and Saral, 2011b). This can be attributed to the presence of phytochemicals such as alkaloids, flavonoids, steroids, terpenoids, saponins and tannins (Vadivel and Panwal, 2016). Furthermore, extracts has also been demonstrated to show aphrodisiac (Kumar et al., 2010), anti-inflammatory, analgesic activity (Mallikarjuna, 2012), wound healing activity (Sumalatha, 2012) and anti-arthritis activity (Sreevaniet al., 2019).

The current work focuses on the chemical and biological synthesis of copper and zinc nanoparticles. The biological synthesis of the nanoparticles is carried out using the ethanolic and hexane extracts of *CrossandraInfundibuliformis*. The produced nanoparticles were then subjected to characterization and comparative evaluation of their antibacterial properties against Gram positive (*S. aureus*, *S. epidermidis*) and negative bacteria (*K. pneumoniae*, *P. aeruginosa*). Further, wound dressing film was developed using synthetic nanoparticles, and their antibacterial ability was assessed.

## 2. Methodology

### 2.1 Materials

*CrossandraInfundibuliformis* was collected from Kozhijamparai, Kerala, India. High-purity chemical reagents were purchased from Himedia, Copper (II) sulphate, Copper acetate, Glacial acetic acid, Zinc nitrate hexahydrate ( $ZnNO_3 \cdot 6H_2O$ ), sodium hydroxide (NaOH),  $CuC_{12}H_{20}O$ , Zinc sulphate.

### 2.2 Preparation of *CrossandraInfundibuliformis* extract

The flowering branch of *CrossandraInfundibuliformis* was utilized for the extraction procedure, wherein 5 g of finely grounded samples were packed in soxhlet extraction unit and extracted using 100 mL of distilled water at 60 °C for 12 hrs. The extract was completely dried in water bath at 40 °C and subsequently stored at 4 °C till further analysis (Sharmila and Gomathi, 2011).

### 2.3 Preparation of nanoparticles (Chemical and biosynthesis)

#### 2.3.1 Synthesis of Copper Oxide Nanoparticles

The biosynthesis of Copper oxide (CO) nanoparticles from the *CrossandraInfundibuliformis* extract was initiated through drop wise addition of the plant extract into 20 mL of aqueous copper sulphate solution maintained under constant stirring at 100 °C. The samples were incubated for 24 hours in dark with vigorous stirring, wherein the initial deep blue coloration shifts to dark red (Abboud et al., 2014).

The CO nanoparticles (CO-NP) through chemical route were synthesized using Copper acetate as precursor and sodium hydroxide as the reducing agent. In brief, 100 mL of 0.2 M copper acetate solution was added with 0.3 mL of glacial acetic acid in a round bottom flask and allowed to boil with continuous stirring. Subsequently, 5 mL of 6 M sodium hydroxide solution was introduced to the flask, wherein an instant color shift from blue to black was observed. Following three hours of continued reaction under the same conditions, the mixture was cooled to room temperature. The solution was centrifuged at 12,000 rpm for 20 min and the resulting precipitate obtained was washed subsequently with distilled water and ethanol. Thereafter, the samples were kept at 60 °C for 6 hrs to attain the dried CO-NP (Ahamed et al., 2014).

#### 2.3.2 Synthesis of Zinc Oxide nanoparticles

The biosynthesis of Zinc oxide (ZO) nanoparticles was initiated through addition of 10 mL *CrossandraInfundibuliformis* extract to 90 mL of zinc sulphate solution (0.3 M) and stirred consistently for 6 hrs at 80 °C. After turning opaque and transforming into brown color, the solution was left to dry at 110 °C. The retained powder was calcined in a furnace for 2hrs at 600 °C (Miri et al., 2019).

The ZO-NP synthesis via chemical process was facilitated through gradual addition of ammonium hydroxide into 0.2 M zinc chloride solution. The reaction was stirred continuously at room temperature till precipitation is attained. After centrifuging the mixture for 10 min at 12,000 rpm, the precipitate was

washed with distilled water. Thereafter, it was dried at 100 °C and subsequently calcined at 450 °C for 2 hrs (Srivastava et al., 2013).

## 2.4 Characterization of *Crossandrafundibuliformis* extract

The synthesized nanoparticle's (CO-NP & ZO-NP) optical characteristics were ascertained by UV Visible spectroscopy within the 280–420 nm range (Cary-8454 spectrophotometer). The stability of the synthesized nanoparticles was verified by measuring their zeta potential (CAD, Zeta Compact), and their particle size was determined using dynamic light scattering analysis (Nano-Sizer, Vasco3, Cordouan) (Yedurkar et al., 2016).

## 2.5 Antibacterial potential of the synthesized nanoparticles

### 2.5.1 Antibacterial activity

The agar diffusion technique was used to investigate the antibacterial activity of synthesized CO-NP and ZO-NP. The test organisms comprised of *S. aureus*, *S. epidermidis*, *K. pneumoniae* and *P. aeruginosa* and their pure cultures were uniformly swabbed onto individual Muller Hinton agar plates using sterile cotton swabs. The wells were cut on the agar surface of each plate using a 6 mm borer. The wells were loaded with 20 µL of the nanoparticle solution (10 µg/µL) and the plates were allowed to air dry. Thereafter, the plates were incubated for 24 hrs at 37 °C and different levels of zone of inhibition were measured (Velmathi et al., 2010).

### 2.5.2 Determination of MIC

The minimum concentration of the synthesized nanoparticles necessary to exhibit the antibacterial activity was established through the standard broth dilution assay. The samples were diluted serially (two-fold dilution) at concentration ranging from 5 mg/mL to 0.00975 mg/mL in the Muller Hinton broth and inoculated with the test organisms (*S. aureus*, *S. epidermidis*, *K. pneumoniae* and *P. aeruginosa*) at 10<sup>8</sup> CFU/ml (0.5 McFarland's standard). The samples were then incubated for 24 hrs at 37 °C and the minimum inhibitory concentration was determined as the lowest concentration at which no visible growth was observed (Parvekar et al., 2020).

### 2.5.3 Determination of MBC

The least concentration of nanoparticles required to kill the bacteria was determined by inoculating 100 µL of the samples from MIC that exhibited no visible bacterial growth onto Muller Hinton agar and incubated for 24 hrs at 37 °C (Parvekar et al., 2020).

## 2.6 Preparation and application of wound dressing film

Wound dressing material was prepared by incorporating the synthesized nanoparticles (CO-NP and ZO-NP) into the polyvinyl alcohol (PVA) film matrix. The polyvinyl alcohol (2 % w/v) was mixed with distilled and stirred at room temperature. The nanoparticle suspension corresponding to 200 µg/µL concentration was added drop wise to the PVA solution, and was subsequently followed up with 2 % citric acid (v/v) addition. The solution was stirred for 30 min at room temperature and thereafter poured incubated overnight at 60 °C in a plastic petri dish. The antibacterial potential of the developed film was assessed by placing the developed nanocomposite film onto the above *S. aureus* and *K. pneumoniae* swabbed Muller Hinton agar plates. The plates were incubated at 37 °C for 24 hrs (Bagyaraj et al., 2021).

## 2.7 Statistical analysis

GraphPad Prism 5 was used for statistical analysis, and two-way ANOVA was used to examine the statistical comparisons of multi-group data. Statistically significant values were defined as  $*p < 0.05$ . The findings were displayed as mean  $\pm$  SD, and each test was run in triplicate.

## 3. Results and Discussion

### 3.1 Synthesis of Copper Oxide and Zinc oxide nanoparticles

The copper ions reduction to copper oxide nanoparticles can be attributed through the change in color of the reaction mixtures from light to dark brown (Fig 1a). In the biological synthesis, the extract of *Crossandrafundibuliformes* reduces metal ions and serves as a stabilizing agent to regulate the size and shape of the generated nanoparticles (Din et al., 2017). The presence of the flavonoid content is often attributed to release of hydrogen atom that could impart tautomeric changes due to the enol to keto forms by reduction of the copper sulfate to copper oxide nanoparticle. The presence of flavonoids is frequently associated with the release of hydrogen atoms, which could impart tautomeric change due to the enol to keto forms through the reduction of copper sulfate to copper oxide nanoparticle (Jacobs et al., 2010). This confirms that extract from *Crossandrafundibuliformes* could synthesis copper oxide nanoparticles at room temperature and pressure without the need of chemicals, surfactants, or polymers. The chemical process begins with the development of copper hydroxide, which, upon continuous boiling, facilitates the removal of water molecules, thereby resulting in copper oxide nanoparticles (Sharma et al., 2020).

The biological technique for producing zinc oxide nanoparticles also involves using extracts from *Crossandrafundibuliformes* as stabilizing and reducing agents. Zinc ions are reduced by the bioactive components in the *Crossandrafundibuliformes* extracts to zinc hydroxide, which then produces zinc oxide nanoparticles when it is calcined. The alternate scenario is the reduction of zinc metal ions to the zinc zero valence state, which is subsequently calcined to produce zinc oxide (36). The synthesized zinc oxide nanoparticles are shown in Fig 1b. The chemical synthesis process involves the formation of white to colored zinc hydroxide precipitate which upon the thermal decomposition process forms zinc oxide nanoparticles (Srivastava et al., 2013).

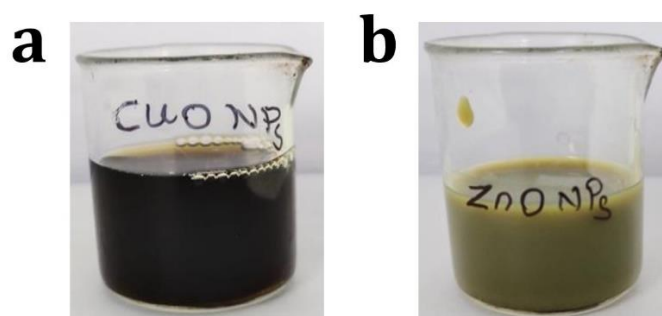


**Fig 1: Synthesis of nanoparticles: a. Copper oxide and b. Zinc oxide**

### 3.2 Characterization of the synthesized nanoparticles

The optical absorption spectrum of copper and zinc oxide nanoparticles recorded between the range of 280-420 nm revealed an absorbance peak of 574 nm and 333 nm, respectively (Fig 2a, b). This peak is caused by an electron transfer from valence to conduction band in the synthesized metal oxide

nanoparticles (CO-NP & ZO-NP) (Miri et al., 2019). The particle size switching to the SPR band wavelength determines the optical characteristics of metal oxides (Jadhav et al., 2011).

Further, this also substantiates the role of *Crossandrafundibuliformes* as a reducing agent for nanoparticle synthesis. Copper nanoparticles have been shown to have an absorption band between 550 and 600 nm. The copper particles had a high at 574 nm that progressively turned yellowish brown, signifying that the copper was oxidizing from its zero to its +2-oxidation state. However, their mildly extended size distribution can be correlated with the slightly broad peak obtained around at 574 nm (Gharibshahi&Saion, 2012). Conversely, the excitation of valence electrons organized in the ZO-NP produced a strong peak at 333 nm (Huang et al., 2006). Herein, the sharp peak obtained corresponds to the narrow size distribution of the synthesized ZO-NP.

The Dynamic Light Scattering approach was utilized to determine the hydrodynamic size of synthesized nanoparticles by considering each particle as a distinct sphere in the Brownian movement. The size distribution of the nanoparticles synthesized through biological and chemical routes are presented in Fig 2c, d, e, f. The results revealed that the CO-NP developed through biological and chemical route exhibited size distribution in the range between 20 nm to 80 nm and 10 nm to 80 nm, respectively. The maximum size distribution was found to be around 50 nm for both the methods. Similarly, the size distribution for ZO-NP nanoparticles was found to be 20 nm to 70 nm for both biological and chemical methods. Correspondingly, the maximum size distribution was found to be 40 nm for nanoparticles synthesized by both strategies.

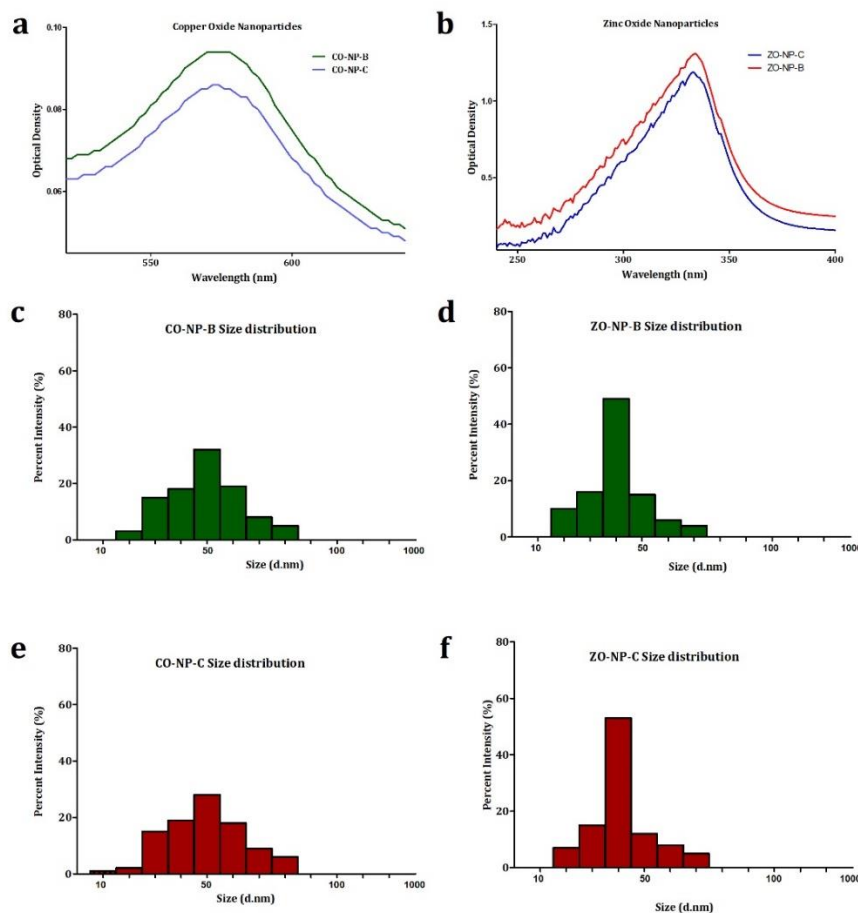


**Fig 2: Characterization of nanoparticles: a.** UV spectroscopic analysis of copper oxide nanoparticles, **b.** UV spectroscopic analysis of zinc oxide nanoparticles, **c.** DLS size distribution analysis of biogenic

copper oxide nanoparticles, **d.** DLS size distribution analysis of biogenic zinc oxide nanoparticles, **e.** DLS size distribution analysis of chemically synthesized copper oxide nanoparticles and **f.** DLS size distribution analysis of chemically synthesized zinc oxide nanoparticles.

### 3.3 Antibacterial potential of synthesized nanoparticles

#### 3.3.1 Determination of zone of inhibition

The zone of inhibition evaluation for the synthesized CO-NP and ZO-NP through both biological and chemical methods are given in table 1. The highest activity for biosynthesis was displayed by ZO-NP against *K. pneumoniae*, followed by *S. epidermidis*, *S. aureus* and *P. aeruginosa* with 37 mm, 33 mm, 32 mm and 16 mm, respectively at 10 µg/µL concentration. Likewise, the CO-NP exhibited highest activity against *K. pneumoniae*, followed by *S. epidermidis*, *S. aureus* and *P. aeruginosa* with 22 mm, 15 mm, 15 mm and 13 mm at the same concentration (Fig 3). The chemical route synthesis nanoparticles demonstrated antibacterial activity similar to those produced by the biosynthesis nanoparticles.

The CO-NP and ZO-NP's antibacterial action can potentially be facilitated through several mechanisms, such as protein denaturation, intracellular disruption, reactive oxygen species, cell membrane degradation, and metal ion release (Slavin et al., 2017b). The CO-NP tends to show prominent antibacterial action against *S. aureus*, *P. aeruginosa* (Usman et al., 2013), *K. pneumoniae* (Mahapatra et al., 2008) and *S. epidermidis* (Bhavyasree & Xavier, 2022). Likewise, the ZO-NP also displays significant activity towards *S. aureus*, *P. aeruginosa*, *S. epidermidis* and *K. pneumoniae* (Sirelkhatim et al., 2015; Da Silva et al., 2019).

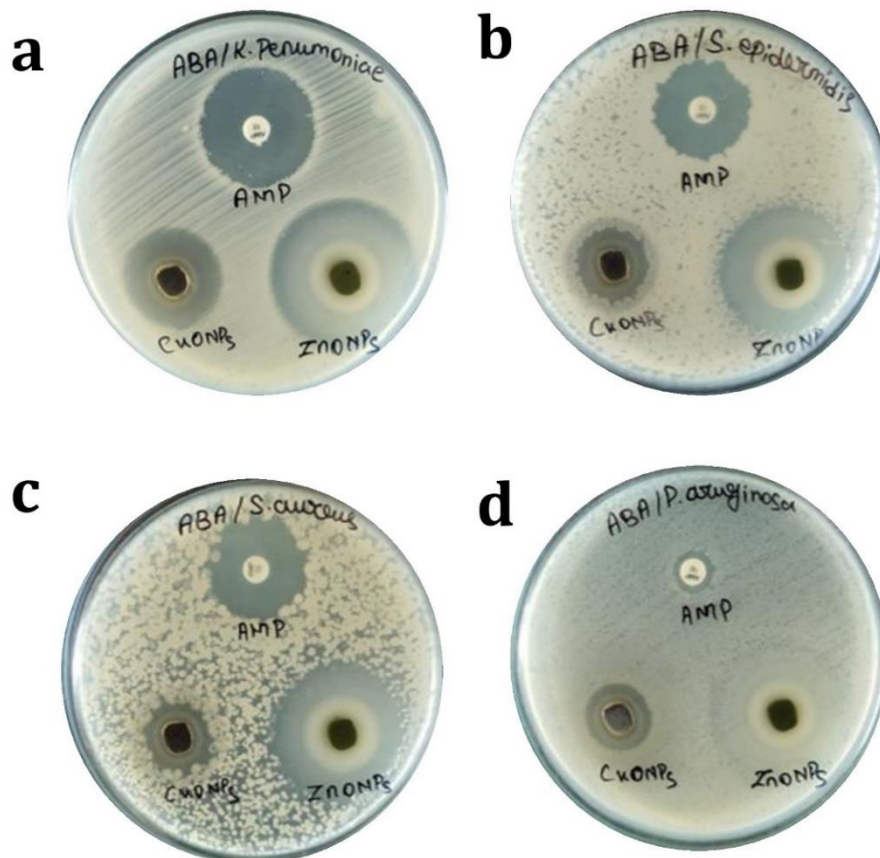


**Fig 3: Determination of zone of inhibition: a.** Zone of inhibition of *K. pneumoniae*, **b.** Zone of inhibition of *S. epidermidis*, **c.** Zone of inhibition of *S. aureus* and **d.** Zone of inhibition of *P. aeruginosa*.

### 3.3.2 Determination of MIC

The MIC of produced CO-NP and ZO-NP (both biological and chemical) was established by the amount of growth inhibition that these compounds inflicted on *S. aureus*, *S. epidermidis*, *K. pneumoniae* and *P. aeruginosa* at its lowest concentrations. The tubes comprising of CO-NP was found to show no turbidity, thereby exhibiting inhibition of growth at 7.8 µg/µL for *S. aureus* and *S. epidermidis*, while 31.25 µg/µL for *P. aeruginosa* and 15.6 µg/µL for *K. pneumoniae*. Similarly, the ZO-NP exhibited MIC of 1.95 µg/µL for *K. pneumoniae*, 3.9 µg/µL for *S. epidermidis*, 7.8 µg/µL for *S. aureus* and 15.6 µg/µL for *P. aeruginosa* (Fig 4).

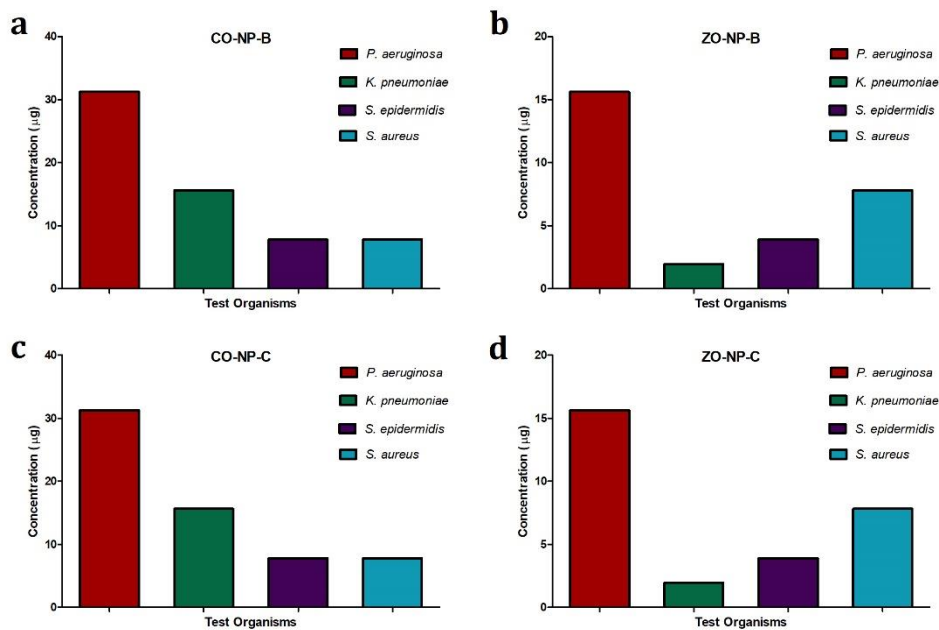


**Fig 4: Determination of minimum inhibitory concentration (MIC) of nanoparticles: a.** MIC analysis of biogenic copper oxide nanoparticles, **b.** MIC analysis of biogenic zinc oxide nanoparticles, **c.** MIC analysis of chemically synthesized copper oxide nanoparticles and **d.** MIC analysis of chemically synthesized zinc oxide nanoparticles.

### 3.3.3 Determination of MBC

The 100 µL of suspension from non-turbid MIC test tubes of CO-NP (biosynthesis) upon plating displayed no growth at concentrations of 15.6 µg/µL for *S. epidermidis* and *S. aureus*, 62.5 µg/µL for *P. aeruginosa* and 31.25 µg/µL for *K. pneumoniae*. Likewise, the ZO-CP (biosynthesis) showed no growth after plating at concentration of 3.9 µg/µL for *K. pneumoniae*, 7.8 µg/µL for *S. epidermidis*, 15.6 µg/µL for *S. aureus* and 31.25 µg/µL for *P. aeruginosa*. The CO-NP and ZO-NP synthesized through chemical routes also exhibited similar results as could be compared from Fig 5.

**Table 1: Zone of inhibition for nanoparticles**

S. No	Organism	CO-NP-B (mm)	ZO-NP-B (mm)	CO-NP-C (mm)	ZO-NP-C (mm)
1.	<i>P. aeruginosa</i>	13	16	12	15
2.	<i>K. pneumoniae</i>	22	37	21	36
3.	<i>S. epidermidis</i>	15	33	15	33
4.	<i>S. aureus</i>	15	32	16	31

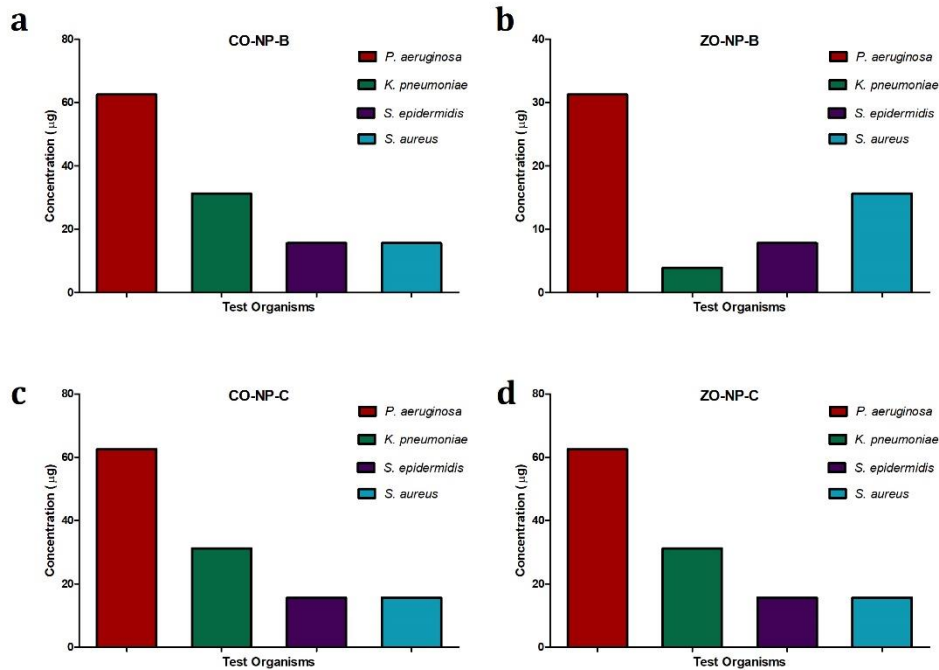


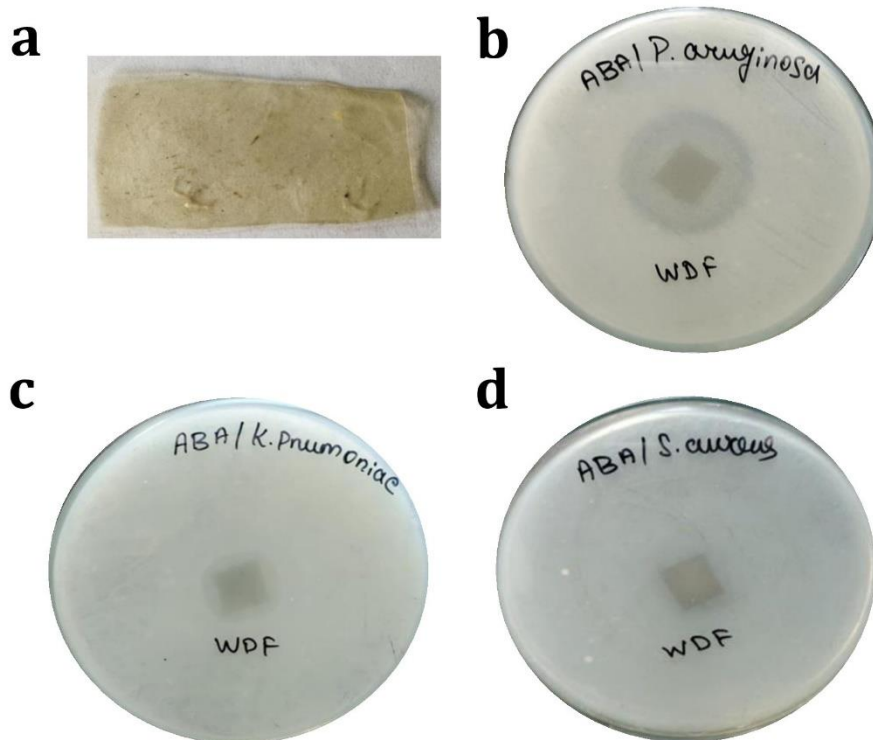
**Fig 5: Determination of minimum bactericidal concentration (MBC) of nanoparticles: a.** MBC analysis of biogenic copper oxide nanoparticles, **b.** MBC analysis of biogenic zinc oxide nanoparticles, **c.** MBC analysis of chemically synthesized copper oxide nanoparticles and **d.** MBC analysis of chemically synthesized zinc oxide nanoparticles.

### 3.4 Preparation and application of wound dressing film

The application of the prepared wound dressing film (Fig 6a) to exert antibacterial activity against the target bacteria was evaluated by observing their inhibitory zone. It is evident from Fig 6b that the nanocomposite films had a good antibacterial effect against the test pathogens. The inhibitory zone diameters for CO-NP (biosynthesized) based films were 32 mm for *P. aeruginosa*, 13 mm for *S. epidermidis*, 11 mm for *S. aureus* and 10 mm for *K. pneumoniae*. Likewise, ZO-NP (biosynthesized) films exhibits zone of inhibition of 35 mm for *P. aeruginosa*, 17 mm for *S. epidermidis*, 14 mm for *S. aureus* and 11 mm for *K. pneumoniae*. The CO-NP synthesized through chemical method displayed a zone of inhibition of 31 mm, 14 mm, 12 mm and 09 mm for *P. aeruginosa*, *S. epidermidis*, *S. aureus* and *K. pneumoniae*, respectively. Similarly, the ZO-NP (chemical method synthesis) films showed zone of inhibition of 33 mm, 15 mm, 13 mm and 11 mm for *P. aeruginosa*, *S. epidermidis*, *S. aureus* and *K. pneumoniae*, respectively (Table 2).

**Table 2: Application of wound dressing film**

S. No	Organism	CO-NP-B (mm)	ZO-NP-B (mm)	CO-NP-C (mm)	ZO-NP-C (mm)
1.	<i>P. aeruginosa</i>	32	35	31	33
2.	<i>K. pneumoniae</i>	10	11	09	11
3.	<i>S. epidermidis</i>	13	17	14	15
4.	<i>S. aureus</i>	11	14	12	13



**Preparation of nanoparticle incorporated wound dressing film and zone of inhibition assay:** **a.** Wound dressing film incorporated with copper oxide nanoparticle, **b.** Zone of inhibition analysis of biogenic copper oxide nanoparticle incorporated wound dressing film against *P. aeruginosa*, **c.** Zone of inhibition analysis of biogenic copper oxide nanoparticle incorporated wound dressing film against *K. pneumoniae* and **d.** Zone of inhibition analysis of biogenic copper oxide nanoparticle incorporated wound dressing film against *S. aureus*.

### Conclusion

The present work demonstrates the efficacy of nanoparticles synthesized through biogenic route and also displayed considerable antibacterial potential. The green synthesis offers several advantages over the presently employed chemical methods, such as being ecofriendly, acting simultaneously as reducing, capping and stabilizing agent, ease of synthesis etc. With its potential for producing various metals and metal oxide nanoparticles, this biosynthetic approach holds promise for use in biotechnological, medicinal, environmental, and biotechnological applications.

### Acknowledgements

The authors would like to express sincerest gratitude to the Institutions, Hindusthan College of Arts & Science and Dr. NGP Arts & Science College, Coimbatore for providing all the resources to carry out the work. The authors are thankful to the technicians from Hindusthan College of Arts & Science and Dr. NGP Arts & Science College, Coimbatore for their consistent support in execution of the experiments.

### References

1. Abboud, Y.; Saffaj, T.; Chagraoui, A.; Bouari, A. E.; Brouzi, K.; Tanane, O.; and Ihssane, B. (2013). Biosynthesis, characterization and antimicrobial activity of copper oxide nanoparticles (CONPs)

- produced using brown alga extract (Bifurcariabifurcata). *Applied Nanoscience*, 4(5), 571–576. <https://doi.org/10.1007/s13204-013-0233-x>.
- Ahamed, M.; Alhadlaq, H. A.; Khan, M. A. M.; Karuppiah, P.; and Al-Dhabi, N. A. (2014). Synthesis, characterization, and antimicrobial activity of copper oxide nanoparticles. *Journal of Nanomaterials*, 2014, 1–4. <https://doi.org/10.1155/2014/637858>.
  - Ahmad, F.; Ashraf, N.; Ashraf, T.; Zhou, R.-B.; and Yin, D. (2019). Biological synthesis of metallic nanoparticles (MNPs) by plants and microbes: their cellular uptake, biocompatibility, and biomedical applications. *Applied Microbiology and Biotechnology*, 103(7), 2913–2935. <https://doi.org/10.1007/s00253-019-09675-5>.
  - Al-saggaf, M. S. (2021). Formulation of insect chitosan stabilized silver nanoparticles with propolis extract as potent antimicrobial and wound healing composites. *International Journal of Polymer Science*, 2021, 1-9. <https://doi.org/10.1155/2021/5578032>.
  - Bagyaraj, S.; Selvam, A. K.; Gomathi, S.; Sandini, S.; Sowmiya, R.; Devi, B. L.; and Vaithyanathan, D. (2021). Preparation and Characterization of Silver Nanoparticle/Aloe Vera Incorporated PCL/PEO matrix for wound dressing application. *Indian Journal of Biochemistry & Biophysics*. <https://doi.org/10.56042/ijbb.v58i1.40324>.
  - Batool, M.; Khurshid, S.; Qureshi, Z.; and Daoush, W. M. (2020). Adsorption, antimicrobial and wound healing activities of biosynthesised zinc oxide nanoparticles. *Chemical Papers*, 75(3), 893–907. <https://doi.org/10.1007/s11696-020-01343-7>.
  - Bhavyasree, P. G.; and Xavier, T. S. (2022). Green synthesised copper and copper oxide based nanomaterials using plant extracts and their application in antimicrobial activity: Review. *Current Research in Green and Sustainable Chemistry*, 5, 100249. <https://doi.org/10.1016/j.crgsc.2021.100249>.
  - Boateng, J.; and Catanzano, O. (2015b). Advanced Therapeutic Dressings for Effective Wound Healing—A Review. *Journal of Pharmaceutical Sciences*, 104(11), 3653–3680. <https://doi.org/10.1002/jps.24610>.
  - Da Silva, B. L.; Abuçafy, M. P.; Manaia, E. B.; Oshiro, J. A.; Chiari-Andréo, B. G.; and Pietro, R. C. L. R. (2019). Relationship Between Structure and Antimicrobial Activity Of Zinc Oxide Nanoparticles: An Overview. *International Journal of Nanomedicine*, Volume 14, 9395–9410. <https://doi.org/10.2147/ijn.s216204>.
  - Dave, S.; Patel, K.; Patel, P.; Bhattacharya, I.; Gangwane, A.; and Thakur, A. (2021). Phytochemical screening and Antimicrobial activity of *Crossandra Infundibuliformis*. *Annals of the Romanian Society for Cell Biology*, 25(6), 20408-20414. <https://www.annalsofrscb.ro/index.php/journal/article/view/10096>
  - Din, M. I.; Arshad, F.; Hussain, Z.; and Mukhtar, M. (2017). Green adeptness in the synthesis and stabilization of copper nanoparticles: catalytic, antibacterial, cytotoxicity, and antioxidant activities. *Nanoscale Research Letters*, 12(1). <https://doi.org/10.1186/s11671-017-2399-8>.
  - Elamathi, R.; Deepa, T.; Kavitha, R.; Kamalakannan, P.; Sridhar, S.; and Suresh Kumar, J. (2011). Phytochemical screening and antimicrobial activity of leaf extracts of *Crossandra infundibuliformis* (L.) nees on common bacterial and fungal pathogens. *International journal of current research*. 1, 72-77.

13. Ficai, D.; Oprea, O.; Ficai, A.; and Holban, A. M. (2014). Metal oxide nanoparticles: Potential uses in biomedical applications. *Current Proteomics*, 11(2), 139–149. <https://doi.org/10.2174/157016461102140917122838>.
14. Gharibshahi, E.; and Saion, E. (2012). Influence of dose on particle size and optical properties of colloidal platinum nanoparticles. *International Journal of Molecular Sciences*, 13(12), 14723–14741. <https://doi.org/10.3390/ijms131114723>.
15. Gil, E. S.; Panilaitis, B.; Bellas, E. and Kaplan, D. L. (2012). Functionalized silk biomaterials for wound healing. *Advanced Healthcare Materials*, 2(1), 206–217. <https://doi.org/10.1002/adhm.201200192>.
16. Gupta, B.; Agarwal, R.; and Alam, M. S. (2010). Textile-based smart wound dressings. *Indian Journal of Fiber and Textile Research*, 35, 174–187. <http://nopr.niscair.res.in/handle/123456789/9766>.
17. Huang, G. G.; Wang, C.-T.; Tang, H.-T.; Huang, Y.-F.; and Yang, J. (2006). ZNO Nanoparticle-Modified Infrared internal reflection elements for selective detection of volatile organic compounds. *Analytical Chemistry*, 78(7), 2397–2404. <https://doi.org/10.1021/ac051930>.
18. Jacobs, H. K.; Moalin, M.; Bast, A.; Van Der Vijgh, W. J. F.; and Haenen, G. R. M. M. (2010). An Essential Difference between the Flavonoids MonoHER and Quercetin in Their Interplay with the Endogenous Antioxidant Network. *PLOS ONE*, 5(11), e13880. <https://doi.org/10.1371/journal.pone.0013880>.
19. Jadhav, S. K.; Gaikwad, S. T.; Nimse, M.; and Rajbhoj, A. S. (2011). Copper oxide nanoparticles: synthesis, characterization and their antibacterial activity. *Journal of Cluster Science*, 22(2), 121–129. <https://doi.org/10.1007/s10876-011-0349-7>.
20. Kaya, S.; Cresswell, M.; and Boccaccini, A. R. (2018). Mesoporous silica-based bioactive glasses for antibiotic-free antibacterial applications. *Materials Science and Engineering: C*, 83, 99–107. <https://doi.org/10.1016/j.msec.2017.11.003>.
21. Kumar, A., Sumalatha, K. R., & Lakshmi, S. (2010). Aphrodisiac Activity of *Crossandra in fundibuliformis* (L.) on Ethanol Induced Testicular Toxicity in Male Rats. *Pharmacologyonline*, 2, 812–817. <https://pharmacologyonline.silae.it/files/archives/2010/vol2/079.Kumar.pdf>.
22. Lemire, J.; Harrison, J. J.; and Turner, R. J. (2013). Antimicrobial activity of metals: mechanisms, molecular targets and applications. *Nature Reviews Microbiology*, 11(6), 371–384. <https://doi.org/10.1038/nrmicro3028>.
23. Li, Q.; Lu, F.; Zhou, G.; Yu, K.; Lu, B.; Xiao, Y.; Dai, F.; Deng-Jun, W.; and Lan, G. (2017). Silver Inlaid with Gold Nanoparticle/Chitosan Wound Dressing Enhances Antibacterial Activity and Porosity, and Promotes Wound Healing. *Biomacromolecules*, 18(11), 3766–3775. <https://doi.org/10.1021/acs.biomac.7b01180>.
24. Madhumitha, G.; and Saral, A. M. (2011b). Preliminary phytochemical analysis, antibacterial, antifungal and anticandidal activities of successive extracts of *Crossandra in fundibuliformis*. *Asian Pacific Journal of Tropical Medicine*, 4(3), 192–195. [https://doi.org/10.1016/s1995-7645\(11\)60067-9](https://doi.org/10.1016/s1995-7645(11)60067-9).
25. Mahapatra, O.; Bhagat, M.; Gopalakrishnan, C.; and Arunachalam, K. D. (2008). Ultrafine dispersed CuO nanoparticles and their antibacterial activity. *Journal of Experimental Nanoscience*, 3(3), 185–193. <https://doi.org/10.1080/17458080802395460>.

26. Mallikarjuna, M. (2012). The Analgesic and Anti-inflammatory Activities of the Leaf Extract of *CrossandraInfundibuliformis*. *International Journal of Innovative Pharmaceutical Research*, 3(2), 203-207.
27. Martinotti, S.; and Ranzato, E. (2018). Honey, wound repair and regenerative medicine. *Journal of Functional Biomaterials*, 9(2), 34. <https://doi.org/10.3390/jfb9020034>.
28. Miri, A.; Mahdinejad, N.; Ebrahimi, O.; Khatami, M.; and Sarani, M. (2019). Zinc oxide nanoparticles: Biosynthesis, characterization, antifungal and cytotoxic activity. *Materials Science and Engineering: C*, 104, 109981. <https://doi.org/10.1016/j.msec.2019.109981>.
29. Niska, K.; Zielińska, E.; Radomski, M. W.; and Inkielewicz-Stepniak, I. (2018). Metal nanoparticles in dermatology and cosmetology: Interactions with human skin cells. *Chemico-Biological Interactions*, 295, 38–51. <https://doi.org/10.1016/j.cbi.2017.06.018>.
30. Parvekar, P.; Palaskar, J.; Metgud, S.; Maria, R.; and Dutta, S. D. (2020). The minimum inhibitory concentration (MIC) and minimum bactericidal concentration (MBC) of silver nanoparticles against *Staphylococcus aureus*. *Biomaterial Investigations in Dentistry*, 7(1), 105–109. <https://doi.org/10.1080/26415275.2020.1796674>.
31. Sharma, M.; Sharma, A.; and Majumder, S. (2020). Synthesis, microbial susceptibility and anti-cancerous properties of copper oxide nanoparticles- review. *Nano Express*, 1(1), 012003. <https://doi.org/10.1088/2632-959x/ab9241>.
32. Sharmila, N.; and Gomathi, N. (2011). Antibacterial, Antioxidant activity and Phytochemical studies of *CrossandraInfundibuliformis* leaf extracts. *International Journal of Phytomedicine*, 3, 151–156. <http://arjournals.org/index.php/ijpm/article/download/198/302>.
33. Sirelkhatim, A.; Mahmud, S.; Seeni, A.; Kaus, N. H. M.; Ann, L. C.; Bakhori, S. K. M.; Hasan, H.; and Mohamad, D. (2015). Review on Zinc oxide nanoparticles: antibacterial activity and toxicity Mechanism. *Nano-Micro Letters*, 7(3), 219–242. <https://doi.org/10.1007/s40820-015-0040-x>.
34. Slavin, Y. N.; Asnis, J.; Häfeli, U. O.; and Bach, H. (2017a). Metal nanoparticles: understanding the mechanisms behind antibacterial activity. *Journal of Nanobiotechnology*, 15(1). <https://doi.org/10.1186/s12951-017-0308-z>.
35. Sreevani, S.; Reddy, P. P.; Reddy, C. R.; Sowjanya, A.; and Vinod, G. (2019). In vitro anti-arthritis activity of *crossandraInfundibuliformis* leaf extract. *World Journal of Pharmaceutical Research*, 8 (6), 553-558. [https://wjpr.s3.ap-south-1.amazonaws.com/article\\_issue/1556616426.pdf](https://wjpr.s3.ap-south-1.amazonaws.com/article_issue/1556616426.pdf)
36. Srivastava, V.; Gusain, D.; and Sharma, Y. C. (2013). Synthesis, characterization and application of zinc oxide nanoparticles (n-ZnO). *Ceramics International*, 39(8), 9803–9808. <https://doi.org/10.1016/j.ceramint.2013.04.110>.
37. Sumalatha, K. (2012). Wound healing process and effect of petroleum ether extract of *CrossandraInfundibuliformis* L. Leaf extract in excision wound model. *International Journal of Preclinical and Pharmaceutical Research*, 3(1), 42-49.
38. Thakkar, K. N.; Mhatre, S.; and Parikh, R. Y. (2010). Biological synthesis of metallic nanoparticles. *Nanomedicine: Nanotechnology, Biology and Medicine*, 6(2), 257–262. <https://doi.org/10.1016/j.nano.2009.07.002>.
39. Usman, M.; Zowalaty, M. E. E.; Shameli, K.; Zainuddin, N.; Salama, M. S.; and Ibrahim, N. A. (2013). Synthesis, characterization, and antimicrobial properties of copper nanoparticles. *International Journal of Nanomedicine*, 4467. <https://doi.org/10.2147/ijn.s50837>.

40. Vadivel, E.; and Panwal, S. V. (2016). In vitro anticancer and insecticidal activity of *Crossandra fundibuliformis*. *Journal of Chemical and Pharmaceutical Research*, 8(5), 260-264.
41. Velmathi, S.; Ananthi, N.; Balakrishnan, U.; Babu, M. S.; MubarakAli, D.; and Thajudin, N. (2010). A study on synthesis, characterization, and electrochemical and antibacterial properties of cobalt (II) complexes of Salen-Derived ligands. *Social Science Research Network*. <https://papers.ssrn.com/sol3/Delivery.cfm?abstractid=1694944>.
42. Yang, G.; Zhang, Y.; and Xiao, T. (2012). Preparation and characterization of SnO<sub>2</sub>/ZnO/TiO<sub>2</sub> composite semiconductor with enhanced photocatalytic activity. *Applied Surface Science*, 258(22), 8704–8712. <https://doi.org/10.1016/j.apsusc.2012.05.078>.
43. Yedurkar, S.; Maurya, C. S.; and Mahanwar, P. A. (2016). Biosynthesis of Zinc Oxide Nanoparticles Using *Ixora Coccinea* Leaf Extract—A Green Approach. *Open Journal of Synthesis Theory and Applications*, 05(01), 1–14. <https://doi.org/10.4236/ojsta.2016.51001>.
44. Zhang, W.; Chen, L.; Chen, J.; Wang, L.; Gui, X.; Ran, J.; Xu, G.; Zhao, H.; Zeng, M.; Ji, J.; Li, Q.; Zhou, J.; Ouyang, H.; and Zou, X. (2017b). Silk fibroin biomaterial shows safe and effective wound healing in animal models and a randomized controlled clinical trial. *Advanced Healthcare Materials*, 6(10). <https://doi.org/10.1002/adhm.201700121>.